Journal of Power Sources 221 (2013) 266–271

Contents lists available at SciVerse ScienceDirect

Journal of Power Sources

journal homepage: www.elsevier.com/locate/jpowsour

A high energy and power density hybrid supercapacitor based on an advanced carbon-coated $Li_4Ti_5O_{12}$ electrode

Hun-Gi Jung [a], Nulu Venugopal [a], Bruno Scrosati [a,c,*], Yang-Kook Sun [a,b,*]

[a] Department of WCU Energy Engineering, Hanyang University, Seoul 133-791, South Korea
[b] Department of Chemical Engineering, Hanyang University, Seoul 133-791, South Korea
[c] Department of Chemistry, University of Rome Sapienza, 00185 Rome, Italy

HIGHLIGHTS

- High rate lithium titanium oxide.
- High surface activated carbon.
- Advanced hybrid supercapacitor.
- High energy density and high rate capability.

ARTICLE INFO

Article history:
Received 26 March 2012
Received in revised form
8 August 2012
Accepted 10 August 2012
Available online 21 August 2012

Keywords:
Hybrid supercapacitor
$Li_4Ti_5O_{12}$
Microsphere
High energy density
High power density

ABSTRACT

We describe in this work the synthesis and the characterization of homogeneous, carbon-coated lithium titanium oxide micro spheres and demonstrate their use for the fabrication of an active negative electrode combined with a high surface area, activated carbon positive electrode to form an advanced non aqueous, hybrid supercapacitor. We show that this activated carbon/carbon coated-$Li_4Ti_5O_{12}$ device retains 95% of its initial capacity after 1000 cycles with a maximum volumetric energy and power density of 57 Wh L^{-1} and 2600 W L^{-1}, respectively. Due to this unique performance, the hybrid supercapacitor developed in this work is expected to be a very promising energy storage device suitable for applications that require high energy levels and fast charge and discharge cycles, such as those requested in the EV sector.

1. Introduction

Energy storage technologies are nowadays used in many practical applications including portable electronics, hybrid electric vehicles and military equipment [1–4]. Batteries and electrochemical capacitors (ECs) are the most common types of energy storage systems [2–4]. Li-ion batteries, although costly, have proven to be the power sources of choice for devices requiring energy density values ranging from 120 to 200 Wh kg^{-1} [1–4]. However, due to Li-ion diffusion limits, batteries may have scarce impact for high power application. Electrochemical capacitors, ECs can deliver much higher power than that usually provided by batteries, i.e., about 5 kW kg^{-1} (versus 200 W kg^{-1} of Li-ion batteries) by short time (a few seconds) pulses with good long term stability, however with a much lower energy density [2,3].

To meet the requirements set by many future applications, e.g., Hybrid vehicles (the starters of engines), uninterruptable power supplies (UPS) and handtools etc, it is mandatory to increase the energy density of supercapacitors, if not to the level of lithium batteries, at least to a value several times higher than that offered by the present EC technology. A promising route to arrive at this goal is to move to hybrid supercapacitors, namely devices based on the combination of high energy battery electrodes with common electrochemical double layer capacitor electrodes, e.g., large surface area activated carbon [4–11].

Among the possible battery materials, lithium titanium oxide, $Li_4Ti_5O_{12}$ (LTO) is known to be the best choice because of its unique properties including high columbic efficiency, thermodynamically stable structure during charge–discharge cycling, minimal solid electrolyte interface and low cost [5–9,12–14]. LTO can in fact support

* Corresponding authors. Department of Chemistry, University of Rome Sapienza, 00185 Rome, Italy. Tel.: +39 06 4991 3530; fax: +39 06 4462 866.
E-mail addresses: Bruno.Scrosati@uniroma1.it (B. Scrosati), yksun@hanyang.ac.kr (Y.-K. Sun).

0378-7753/$ – see front matter
http://dx.doi.org/10.1016/j.jpowsour.2012.08.039

a two-phase electrochemical process with a flat operating voltage of about 1.5 V vs. Li/Li^+ and practically no volume changes during cycling; however, issues such as slow Li^+ ions diffusion coefficient ($<10^{-6}$ cm^2 s^{-1}) and poor electron conductivity (2.65×10^{-7} S cm^{-1}) still prevents the use of LTO in high performance power systems.

A common approach to improve the performance of LTO considers reduction of its particle size to the nanoscale range, so that to achieve reduction of the Li^+ diffusion path [3,7] and finally, to increase the material electrode kinetics. On the other hand, the synthesis of nano LTO particles involves very sensitive experimental procedures with consequent practical difficulties [7,15–17]. In addition, reduction in particle size may lead to a series of negative aspects including: i) an increase in the surface area of the electrode with a consequent enhancement of its reactivity with the electrolyte, leading to side reactions that may seriously affect the cycle life, and ii) a decrease in tap density resulting in a decrease of the volumetric energy density of the device. Another popular approach for upgrading LTO is that of mixing its particles with modified carbon, e.g., carbon nanofibers [7], however, with considerable increase of the net cost of the material; moreover, by this approach, only a part of the LTO primary particles' surface may be in contact with carbon so that to leave the remaining part uncovered and exposed to the electrolyte.

In synthesis, both approaches are not totally valid; hence, considerable effort is spent worldwide to develop advanced, high performance LTO electrodes for application in non-aqueous hybrid supercapacitors. Along this line, we have addressed our research to the development of pitch carbon-coated micron-sized LTO spherical particles, namely to a morphology that is expected to lead to a significant improvement of the electrical conductivity of LTO. Indeed, previous work carried out in our laboratory has shown that this carbon-coated LTO has isotropic physical and electrochemical properties that fulfill the high power requirements for Li-ion batteries [18,19]. It is interesting to point out that pitch is a readily available, low-cost carbon providing an efficient source for producing a uniform carbon coating around the LTO micro spheres [18]. All these favorable aspects have encouraged us to extend the use of pitch carbon-coated $Li_4Ti_5O_{12}$ (hereafter simply referred as C-LTO) as a negative electrode to be combined with high surface area, activated carbon (hereafter simply referred as AC) positive electrode for the development of a highly efficient, non-aqueous hybrid supercapacitor (hereafter simply referred as NAHS). The practical relevance of this device is demonstrated by the results reported in this work.

2. Experimental

The pitch carbon-coated $Li_4Ti_5O_{12}$ microsphere particles were synthesized by a previously reported hydrothermal method [18] using highly mesoporous, anatase phase, micron size TiO_2 as precursor [20,21]. High purity $TiCl_4$, urea, and ammonium sulfate were mixed in a distilled water–ethanol mixture in an ice water bath. The homogeneous mixture solution was transferred to a teflon-lined autoclave and heated to a temperature of 393 K for 24 h. After cooling, the resulting slurry was filtered, washed in ethanol, and subsequently subjected to vacuum-drying followed by calcination at 400 °C for 5 h in air. Then, the calcined mesoporous TiO_2 was mixed with a stoichiometric amount of Li_2CO_3 and 20 wt.% pitch as a carbon coating source. This mixture was calcined for 20 h at 900 °C in a furnace purged with Ar at atmospheric pressure. Hereafter, pitch carbon-coated $Li_4Ti_5O_{12}$ is referred to as C-LTO.

3. Material characterization

The morphology, crystalline structure and diffraction data of the synthesized powders were analyzed by field-emission scanning electron microscopy (FE-SEM, model JSM-6400, JEOL), high-resolution transmission electron microscopy (HR-TEM, model JEM-2010, JEOL) and powder X-ray diffraction (XRD, Rigaku Rint-2000 with Cu Kα radiation), respectively. The XRD data were obtained at $2\theta = 10°–80°$, with a step size of 0.03°. The carbon content was measured by elemental analysis using an EA 110 CHNS-O automatic analyzer (CE Instrument). The direct current (DC) electrical conductivity was measured using a direct volt–ampere method (CMT-SR1000, AIT Co.) via sample contact with a four-point probe.

The electrochemical analyses were completed using a half-cell (Li/C-LTO) and a non-aqueous asymmetric hybrid NAHS capacitor (AC/C-LTO). The 2032 coin-type half-cells were assembled with a Li-metal counter electrode and a C-LTO electrode. The electrolyte solution was 1 M $LiPF_6$ in propylene carbonate (Panax Etec Co., Ltd., Korea). The C-LTO electrode was prepared by mixing 80% of the active materials with a 10% carbon black conducting agent (super P and KS6) composite and 10% polyvinylidene difluoride (PVdF) binder in *N*-methyl pyrrolidone. The slurry was coated on a Cu foil (current collector) and dried at 90 °C under vacuum. The thickness of the resulting electrode was 30 μm with the corresponding loading of active material weight about 5.7 mg cm^{-2} (measured electrode density is about 1.7 g cc^{-1}). Charge–discharge tests were performed under constant current (CC) mode between 1.0 and 2.5 V vs. Li/Li^+ at several current densities ranging from 0.17 to 8.5 A g^{-1}. The NAHSs were assembled using the C-LTO as the negative electrode, and activated carbon (AC) as the positive electrode, in a laminated type full cell wrapped in an Al pouch (3×3 cm^2) geometry. The positive electrode was prepared by mixing the activated carbon (Fluka), conductive acetylene black, polytetrafluoroethylene (PTFE), and styrene butadiene rubber (SBR) in a ratio of 78:15:6:1 wt.% with an appropriate amount of solvent ethanol. The mixture was coated on Al foil. The electrodes were dried at 90 °C under vacuum prior to use. The negative electrode (C-LTO) was prepared as aforementioned. The positive and negative electrodes active material weight ratio was close to 5.5:1. This ratio was calculated considering 30 mAh g^{-1} specific capacity for AC [15] and 165 mAh g^{-1} specific capacity for C-LTO. The electrolyte was 1.0 M $LiPF_6$ in propylene carbonate (PC). The specific capacity and electrochemical rate of the cells always refer to the total weight of the active materials in the positive and negative electrodes. Charge–discharge tests were performed in CC-mode at room temperature between the operation voltage widow, 1.5 and 2.5 V at different current densities ranging from 0.17 to 23.4 A g^{-1} using a VMP Potentiostat/Galvanostat (Bio-Logic) operating in galvanostatic mode. For comparative purposes, a conventional AC/AC supercapacitor was assembled and tested using the same electrolyte mentioned before (voltage widow, 0.1–2.3 V).

4. Results and discussion

4.1. Physical properties

The carbon content and the tap density of the C-LTO material developed in this work were determined to be 5.2 wt.% (by CHNS analysis) and 1.31 g cm^{-3} (by tap density analyzer) respectively [18]. The tap density value is 1.5 times more than that of the carbon-free LTO, this being a significant improvement with important implications on the volumetric energy density of the final device employing the C-LTO as electrode material. The detailed surface characteristics and conductivity studies were performed by different analytical measurements, namely BJH pore size distribution, XPS (X-ray Photoelectron Spectroscopy) and four-probe DC method in our previous work on pitch carbon coated LTO prepared by similar synthesis approach [18]. Remarkably, the results revealed that an enormous increase in its electronic

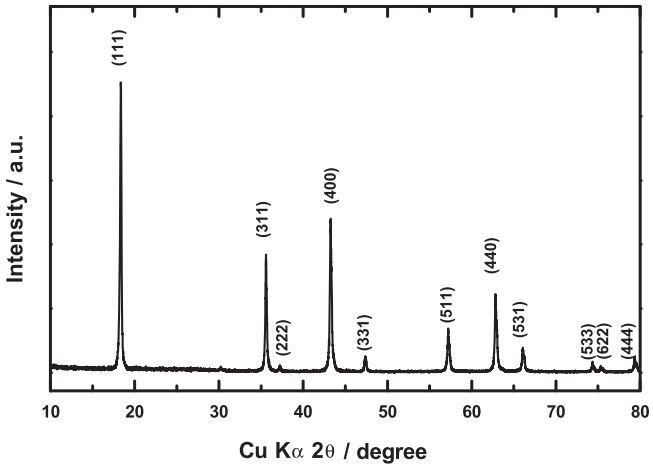

Fig. 1. X-ray diffraction patterns of the C-LTO powders after heat treatment at 900 °C.

conductivity by five orders of magnitude 1.21 × 10^{-2} S cm^{-1}, vs. 2.65 × 10^{-7} S cm^{-1} for carbon-free $Li_4Ti_5O_{12}$, which is achieved from the coated conductive carbon layer and by the in-situ generated mixed valence state of Ti^{3+} and Ti^{4+} within the bulk part of the spherical C-LTO with well-defined mesoporosity (pore diameter ranges from 3 to 10 nm).

Fig. 1 shows the XRD diffraction pattern of the C-LTO powders obtained in this work. The spectrum confirms the cubic spinel structure characteristic of LTO with no evidence of impurity phases. In addition, XRD pattern revealed that carbon was amorphous with no discernable diffractions peaks [22]. The absence of carbon peaks in the XRD diffraction pattern is due to the amorphous nature as was observed for.

Fig. 2 reports the result of a SEM analysis of the C-LTO powders. The image of Fig. 2a reveals that the spherical morphology of the mesoporous TiO_2 precursor was preserved after carbonization with pitch to form the carbon-coated LTO. The higher magnification image of Fig. 2b shows that the spherical LTO powders are composed of 10–50 nm primary particles. It is expected that the Li^+ ions diffusion path is considerably reduced in these nano particles with an associated fast ionic diffusion. Overall, the SEM analysis evidences that the carbon layer is uniformly coated on the LTO surface carbon so to preclude the densification of the primary particles during calcination. The micron scale spherical morphology together with the infiltrated pitch carbon into the each C-LTO particle provides the high tap density.

The carbon distribution throughout LTO particles was investigated by TEM analysis. The cross-sectional TEM image and the corresponding electron energy loss spectroscopy (EELS) carbon mapping are shown in Fig. 3a and b, respectively. The images confirm that the carbon layer is homogeneously coated along the surface of both the primary and the secondary LTO particles. Remarkably, this uniform carbon coating layer enables to increase the electronic conductivity of C-LTO by five orders of magnitude respect to carbon-free LTO, namely from 2.65 × 10^{-7} S cm^{-1} to 1.21 × 10^{-2} S cm^{-1}.

4.2. Electrochemical analysis of half-cell (Li/C-LTO)

Fig. 4 shows typical charge–discharge voltage profiles of the half-cell Li/C-LTO cycled at 1 C. The flat plateau at 1.5 V, corresponding to the Li^+ ion intercalation–deintercalation process in LTO, is clearly displayed [14]. A specific capacity of 163 mAh g^{-1}, which approaches that of 170 mAh g^{-1} theoretical value, is obtained at 1C rate. It is to be noticed that the unique, high performance of our C-LTO directly comes from with its optimized, nano particle size morphology that results in a reduced Li^+ diffusion path and in a high electronic conductivity [15].

Fig. 5 shows the trend of the specific capacity of the Li/C-LTO cell at various current densities. Even at the very high discharge current rate of 50 C (8.5 A g^{-1}), the cell maintained a high capacity of 142 mAh g^{-1}, i.e., 87% of the value delivered at 1 C (0.17 A g^{-1}). Such a high rate capability, that exceeds that of nano-sized LTO and carbon-coated LTO electrodes prepared by differed methods [15,23]. This is an important bonus of our C-LTO electrode in view of its application in NAHSs, see below.

4.3. Electrochemical analysis of hybrid supercapacitor (C-LTO/AC)

The above described favorable properties of the C-LTO encouraged us to explore its use as negative electrode in an advanced NAHS using AC as the positive electrode and a 1 M solution of $LiPF_6$ in propylene carbonate as the electrolyte. The device is shown in scheme in Fig. 6. The working principle is that already reported for similar NAHSs: during electrochemical operation, the electrolyte acts as an ionic source from which the Li^+ cations are intercalated into the C-LTO negative electrode and the PF_6^- anions are adsorbed onto the high surface area AC positive electrode [5,8]. To be effective, the negative electrode must operate with high reversible

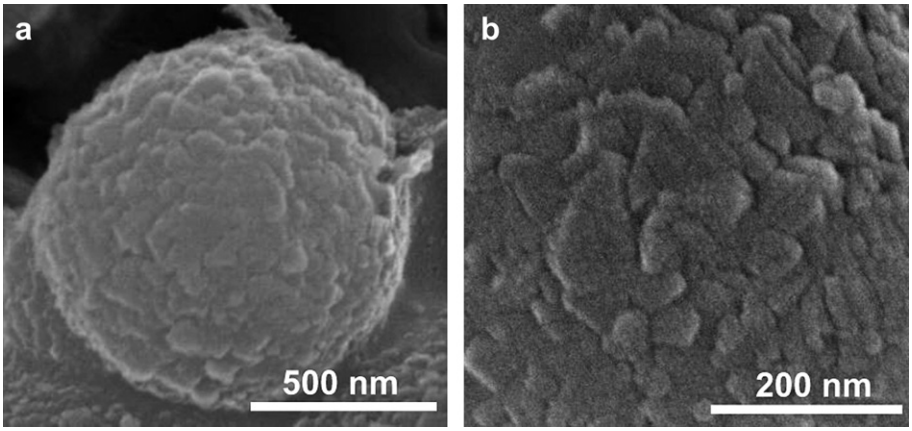

Fig. 2. (a), (b) SEM images of the C-LTO particle: (a) low magnification, (b) high magnification.

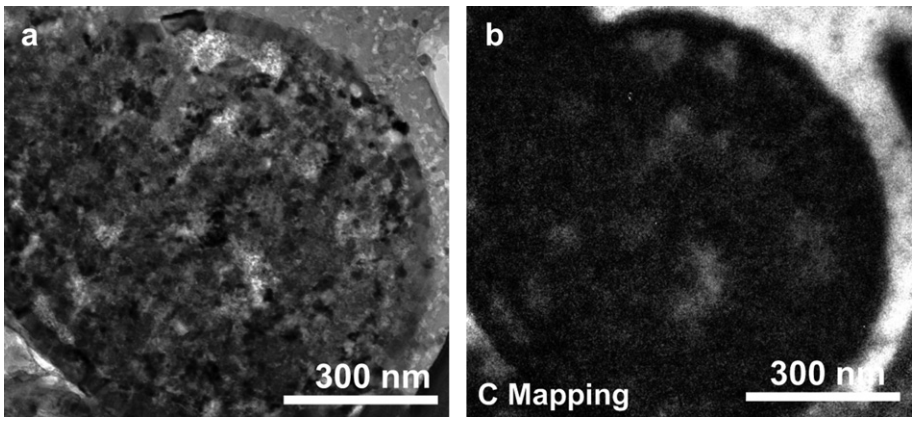

Fig. 3. (a) The cross-sectional TEM image and (b) the corresponding EELS elemental mapping of the carbon.

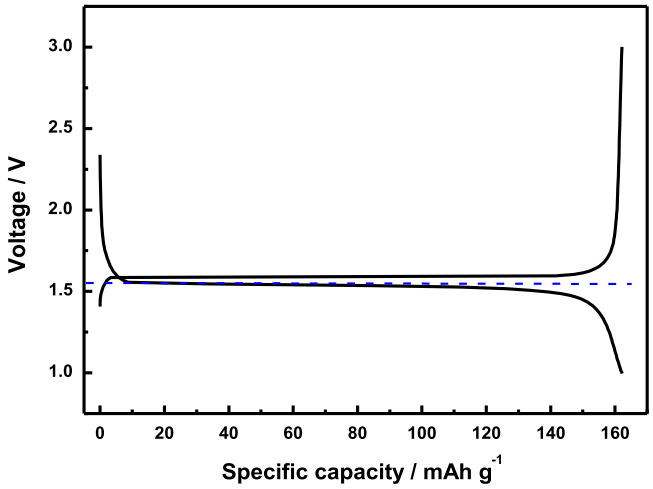

Fig. 4. Charge–discharge curve of the C-LTO electrode. Voltage limits: 1.0 and 3.0 V. Rate: 1 C (0.17 A g^{-1}). Room temperature.

capacity and with a good Li^+ intercalation stability at high current density. On the other hand, the positive electrode material should have high surface area, high reversible capacity at voltages in excess of 0.5 V vs. SHE, and long cycle life. These are in fact the essential conditions for obtaining NAHSs having a specific energy higher than conventional capacitors and specific power greater than batteries. Effectively, commercially available AC materials can satisfy these requirements [4,5,8,9] and the response in lithium half

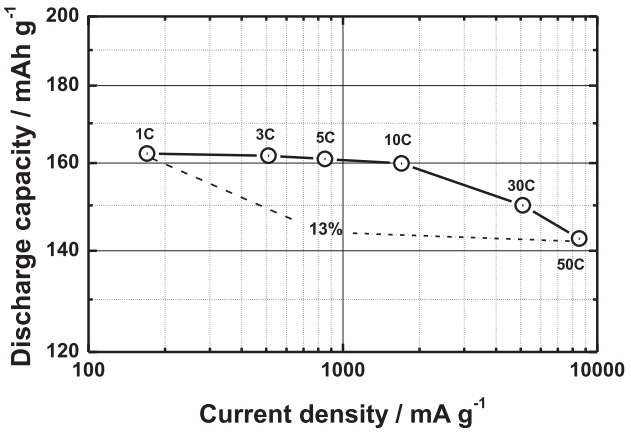

Fig. 5. Discharge capacities of the C-LTO electrode at C-rate values ranging from 1 C (0.17 A g^{-1}) to a 50 C-rate (8.5 A g^{-1}).

cells (see paragraph #2) suggests a similar grading for the C-LTO electrode. In addition, the use of C-LTO shifts the resultant average working voltage of NAHS to a high positive value of 2.25 V, which in turn may contribute to increase the energy density of the device (Fig. 7a). Fig. 7a shows the first charge discharge profiles of the hybrid cell (C-LTO/AC). It is noted that the voltage profiles of C-LTO/AC system is equivalent to the previously obtained in hybrid capacitor systems [15]. On the other hand, linear charge–voltage profile of AC/AC cell (Fig. 7b) represents a typical double layer formation, consistent with previous reports on non-aqueous EDLC systems [5,7].

Fig. 7c shows the response in term of discharge capacity as a function of cycle number of the AC/C-LTO NAHS developed in this

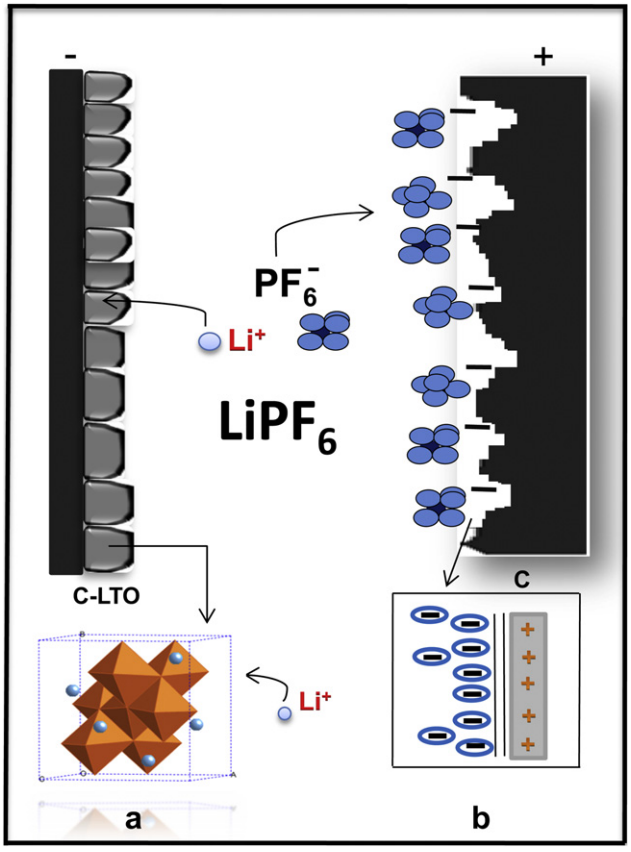

Fig. 6. Schematic illustration of expected electrode reactions in a non-aqueous asymmetric hybrid capacitor. (a) Li-ion intercalation through battery material (C-LTO); (b) electrochemical double layer (EDL) on activated carbon.

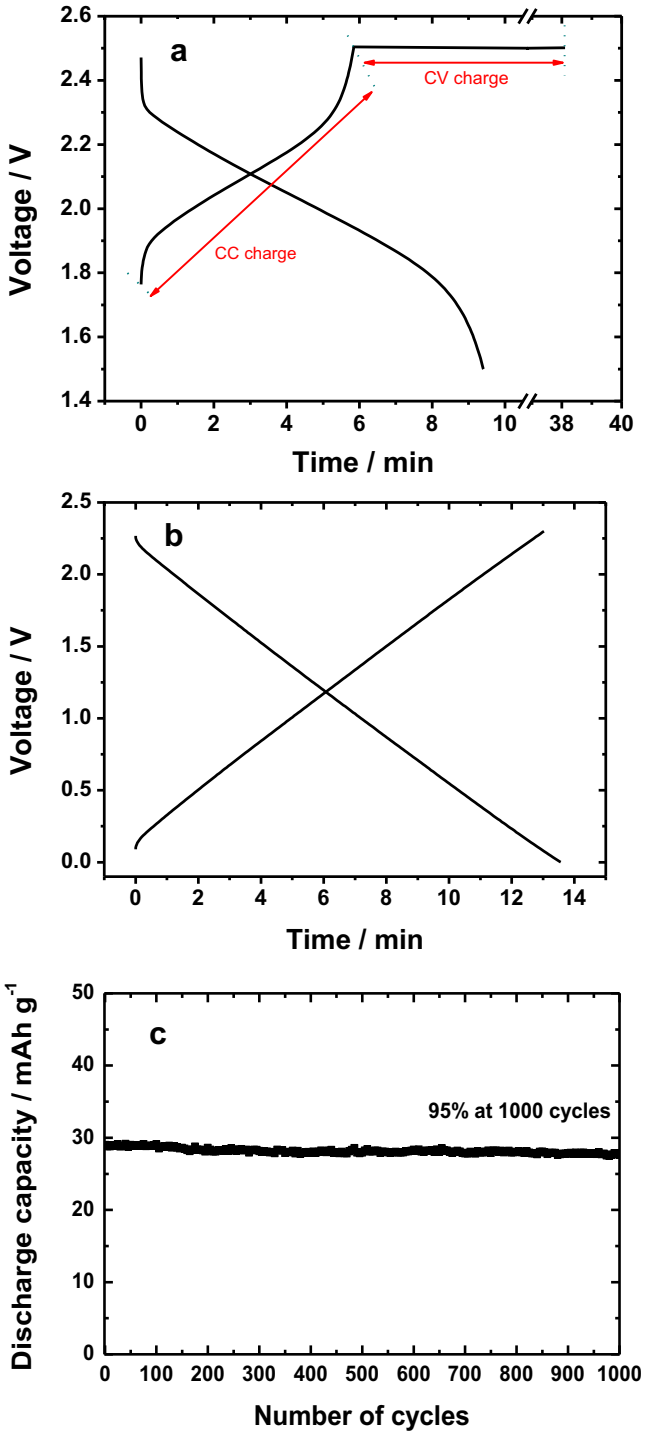

Fig. 7. Charge–discharge curves of the cells tested at 10 C constant rate (a) C-LTO/AC (b) AC/AC. (c) Capacity versus number of cycles of AC/C-LTO NAHS. Rate: 10 C (1.7 A g^{-1}). Room temperature.

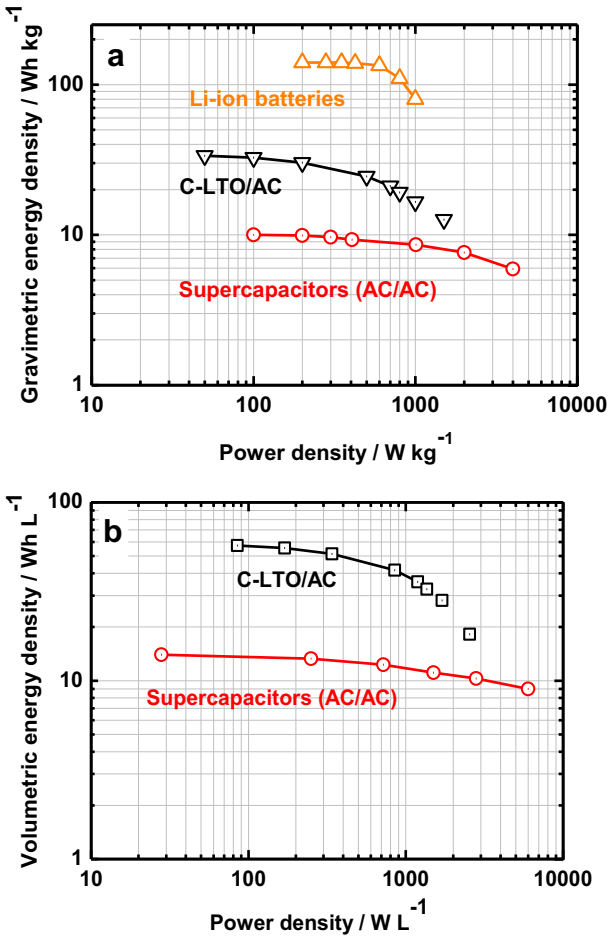

Fig. 8. Ragone plots of hybrid capacitor system (AC/C-LTO). (a) Gravimetric energy and power densities of hybrid capacitor system (AC/C-LTO) vs. conventional supercapacitor system and Li-ion batteries (from Ref. [25]). (b) Volumetric energy and power densities of hybrid capacitor system (AC/C-LTO) vs. supercapacitor system (AC/AC) (from Ref. [7]). The volumetric power and energy densities were calculated based on the electrode density.

work. A stable capacity retention of 95% is obtained after 1000 cycles. This is a relevant result since it demonstrates that our NAHS outstands the performance commonly reported for AC/LTO asymmetric hybrid capacitors [10,15,24]. For instance, considerably lower discharge capacity with poorer retention upon cycling under the same testing conditions have been achieved for comparable AC/LTO NAHS [10,15]. It has to be noted that the key difference is in the morphology of our C-LTO electrode that, as already stressed, allows fast Li^+ ion diffusion and high electronic conductivity. Thus, fast Li^+ intercalation reactions may take place even at very high rates. This fast process at the negative C-LTO is complemented by the prompt non-faradic, anion adsorption one (reversible double-layer mechanism) at the AC positive. Both the anions and the cations are provided by the electrolyte with a cycling process evolving with a steady profile, as shown in Fig. 7c.

Fig. 8 illustrates the Ragone plots obtained for our AC/C-LTO NAHS. The power and energy densities were obtained by discharging the charged device at increasing current densities (starting from 0.17 A g^{-1}) within a potential window of 1.5–2.5 V, and their values are calculated from the generally available methods reported in the literature [10]. For comparative purpose, the data for common supercapacitors and Li-ion batteries are added to plot [7,25]. The maximum energy density obtained from our NAHS is as high as 35.5 Wh kg^{-1} at low current density, see Fig. 7a. Fig. 7b shows the Ragone plot in terms of volumetric energy density, Wh L^{-1}. Due to the high tap density of C-LTO, a remarkable increase in volumetric energy density compared to gravimetric energy density is observed.

5. Conclusion

The results discussed in this work show, by exploiting and advanced, high-rate, carbon-coated, lithium titanium oxide electrode,

that the NAHS here developed offers energy density performances that are higher than those achieved by conventional systems, such as hybrid supercapacitors using polymer materials like poly-fluoro phenyl thiophene (PFPT)/LTO (20 Wh kg^{-1}) [26] or poly-methyl thiophene (PMeT)/LTO (10–14 Wh kg^{-1}) [27], and comparable with those of similar NAHSs [24]. The power density obtained from our device is in fact equal to 1010 W kg^{-1} at a measured energy density of 16 Wh kg^{-1}, which is double that of the conventional electrochemical double layer system, while the power density is comparable to that of an AC/nano-scale LTO system (1000–2000 W kg^{-1} at 10–15 Wh kg^{-1}) [4] and better than that reported for polymer/LTO NAHSs (around 1000 W kg^{-1} at 8–10 Wh kg^{-1}) [4,27]. Even more remarkable is the comparison in terms of volumetric energy density, that is as high as 57 Wh L^{-1} in a low power density range of 10–100 W L^{-1} which is nearly 40% more than the reported value on a similar hybrid capacitor system consisting of nano-sized $Li_4Ti_5O_{12}$ and carbon nano-fiber composite (i.e., 40 Wh L^{-1} at 10–100 W L^{-1}) [7]. In the high power range of 2600 W L^{-1} the proposed NAHS shows volumetric energy density of 18 Wh L^{-1}, i.e., a value almost two times higher than that of conventional EDLC systems [7]. This enhanced volumetric energy density is due to high tap density and the micron-sized negative electrode material, C-LTO developed in this work. Besides that, this much-improved performance with our proposed NAHS system than supercapacitors (AC/AC) and the other capacitors systems (LTO/AC) discussed before is possibly due to the noticed advanced physical properties like improved electronic conductivity, uniformly coated carbon layer and high tap density of C-LTO. Hence, the proposed AC/C-LTO NAHS may be regarded as a very promising energy storage device suitable for applications that require high energy levels and fast charge and discharge cycles, such as those requested in the EV sector.

Acknowledgments

This work was supported by the Human Resources Development of the Korea Institute of Energy Technology Evaluation and Planning (KETEP) grant funded by the Korea government Ministry of Knowledge Economy (No. 20104010100560) and the National Research Foundation of Korea (NRF) grant funded by the Korea government (MEST) (No.2009-0092780).

References

[1] B.E. Conway, Electrochemical Supercapacitors: Scientific Fundamentals and Technological Applications, Kluwer, 1999.
[2] A. Salvatore Aricò, P.G. Bruce, B. Scrosati, J.-M. Tarascon, W.V. Schalkwijk, Nat. Mater. 4 (2005) 366.
[3] M. Winter, R.J. Brodd, Chem. Rev. 104 (2004) 4245.
[4] A.D. Pasquier, I. Plitz, S. Menocal, G.G. Amatucci, J. Power Sources 115 (2003) 171.
[5] G.G. Amatucci, F. Badway, A.D. Pasquier, T. Zheng, J. Electrochem. Soc. 148 (2001) A930.
[6] Y.-G. Wang, Y.-Y. Xia, J. Electrochem. Soc. 153 (2006) A450.
[7] K. Naoi, S. Ishimoto, Y. Isobe, S. Aoyagi, J. Power Sources 195 (2010) 6250.
[8] J.P. Zheng, J. Electrochem. Soc. 150 (2003) A484.
[9] P.A. Nelson, J.R. Owen, J. Electrochem. Soc. 150 (2003) A1313.
[10] C.M. Ionica-Bousquet, D. Munoz-Rojas, W.J. Casteel Jr., R.M. Pearlstein, G.G. Kumar, G.P. Pez, M.R. Palacin, J. Power Sources 196 (2011) 1626.
[11] Y.-G. Wang, J.-Y. Luo, C.-X. Wang, Y.-Y. Xia, J. Electrochem. Soc. 153 (2006) A1425.
[12] E.M. Sorensen, S.J. Barry, H.-K. Jung, J.R. Rondinelli, J.T. Vaughey, K.R. Poeppelmeier, Chem. Mater. 18 (2006) 482.
[13] T. Ohzuku, A. Ueda, N. Yamamoto, J. Electrochem. Soc. 142 (1995) 1431.
[14] M.M. Thackeray, J. Electrochem. Soc. 142 (1995) 2558.
[15] L. Cheng, H.J. Liu, J.J. Zhang, H.M. Xiong, Y.-Y. Xia, J. Electrochem. Soc. 153 (2006) A1472.
[16] A. Guerfi, S. Sevigny, M. Lagace, P. Hovington, K. Kinoshita, K. Zaghib, J. Power Sources 119–121 (2003) 88.
[17] K.N. Jung, S. Pyun, S.W. Kim, J. Power Sources 119–121 (2003) 637.
[18] H.-G. Jung, S.-T. Myung, C.S. Yoon, S.B. Son, K.H. Oh, K. Amine, B. Scrosati, Y.-K. Sun, Energy Environ. Sci. 4 (2011) 1345.
[19] H.-G. Jung, J. Kim, B. Scrosati, Y.-K. Sun, J. Power Sources 196 (2011) 7763.
[20] H.-G. Jung, S.W. Oh, C. Jin, N. Jayaprakash, Y.-K. Sun, Electrochem. Commun. 11 (2009) 756.
[21] H.-G. Jung, C.S. Yoon, J. Prakash, Y.-K. Sun, J. Phys. Chem. C 113 (2009) 21258.
[22] L. Cheng, X.-L. Li, H.-J. Liu, H.-M. Xiong, P.-W. Zhang, Y.Y. Xia, J. Electrochem. Soc. 154 (2007) A692.
[23] J.B. Kim, D.J. Kim, K.Y. Chung, D. Byun, B.W. Cho, Phys. Scr. T139 (2010) 14026.
[24] D. Cericola, P. Novák, A. Wokaun, R. Kötz, J. Power Sources 196 (2011) 10305.
[25] M. Mastragostino, F. Soavi, J. Power Sources 174 (2007) 89.
[26] A.D. Pasquier, A. Laforgue, P. Simon, G.G. Amatucci, J.F. Fauvarque, J. Electrochem. Soc. 149 (2002) A302.
[27] A.D. Pasquier, A. Laforgue, P. Simon, J. Power Sources 125 (2004) 95.